Article

# Chemically Chargeable Photo Battery

Ravikumar Thimmappa,[†] Bhuneshwar Paswan,[†] Pramod Gaikwad,[†]
Mruthyunjayachari Chattanahalli Devendrachari,[†] Harish Makri Nimbegondi Kotresh,[‡]
Ramsundar Rani Mohan,[§] Joy Pattayil Alias,[§] and Musthafa Ottakam Thotiyl*,[†]

[†]Indian Institute of Science Education and Research (IISER) Pune, Dr. Homi Bhabha Road, Pashan, Pune, 411008, India

[‡]Department of Chemistry, Acharya Institute of Technology, Soldevanahalli, Bangalore-560107, India

[§]Physical and Materials Chemistry Division, National Chemical Laboratory (CSIR), Dr. Homibaba Road, Pashan, Pune, 411008, India

**S** *Supporting Information*
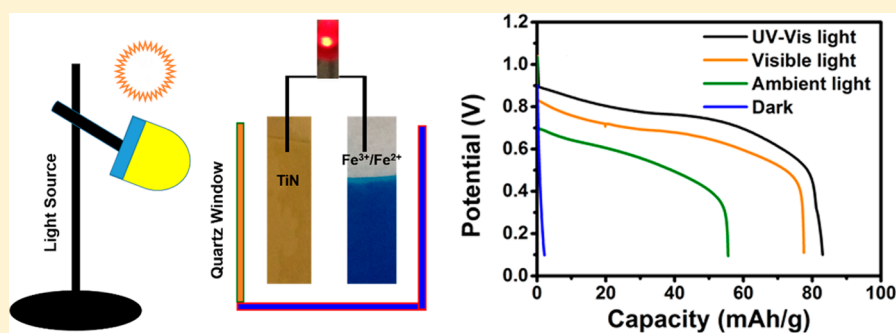
**ABSTRACT:** Here we show a surrogate strategy for power production, wherein light is used to actuate a discharge chemistry in the cathode of an aqueous rechargeable battery (ARB). The proposed photo battery consists of a titanium nitride photoanode, promising cathode material iron(III) hexacyanoferrate(II) as the battery active species and $Na_2S_2O_8$ as the chemical charging agent. The photo battery delivered negligible capacity in the dark and the capacity shot up to 77.8 mAh/g when artificially shined light, confirming that the battery chemistry is light driven. In the ambient light, the device retained 72% of its artificial light discharge capacity with a stable cycling for more than 100 cycles. Further, an unprecedented means for charging the battery rapidly is presented using $Na_2S_2O_8$ and it revitalized the battery in 30 s without any external bias. This methodology of expending a photoanode extends to a battery that is free from dissolution of active materials, irreversible structural changes, spontaneous deinsertion reactions, and safety concerns commonly encountered in the state of the art anode materials in ARBs. Apart from bringing out a sustainable way for power production, this device opens up avenues for charging the battery in the likely events of electrical input unavailability, while solving the crtical issues of longer charging time and higher charging voltage.

## 1. INTRODUCTION

Increased activity across the globe in light harvesting stems from the ever increasing energy consumption and is justified by the faster depletion of fossil fuels and increased greenhouse emissions.[1−4] For human beings to be a sustainable community in terms of energy the ideal solution is harvesting sunlight to produce fuels (water splitting and $CO_2$ reduction) and generate electricity (solar cells).[5−9] Enormous efforts have been put in these areas worldwide to develop durable and economical fuel producing photocatalysts and increasing the efficiency of photovoltaic (PV) and dye sensitized solar cells (DSSC). From the context of energy storage, secondary aprotic metal ion batteries have dominated the market though there are serious issues related to safety, cost, capacity fading, higher charging voltage, longer charging time (of the order of hours), and so on.[10−14] Often, some of these (especially safety and capacity fading) are linked to the stability of the anode materials. Though Li, Na, K, and so on, are attractive anode

materials based on their standard reduction potentials, their incompatibility, and safety concerns with the aqueous (as well as non aqueous) systems have intensified the search for stable, safer, and economical anode materials for aqueous rechargeable batteries (ARBs).[15−19] Conventional carbon-based anodes are unsuitable in ARBs because of their inherent instability in the metal ion inserted state.[17] In ARBs, the existing anode materials lead to siginificant capacity fading due to dissolution of active materials, irreversible structural changes, spontaneous deinsertion reactions, and so on, as pointed out by Kisuk Kang[17] in an excellent review. Recently, in a promising approach, Hanxi Yang has succeeded in introducing an organic type polyimide anode with superior cyclability and stability for ARBs.[18] In a significant development, Yi Cui has brought in a symmetric cell

configuration, wherein they successfully employed manganese hexacyanomanganate open framework as the anode material for ARBs.[19]

In a radically different approach, here we bring in the concept of *light* as the anode for ARBs. We demonstrate that using a photoanode light can be used to actuate a discharge chemistry in the cathode of an ARB and this brings in (1) alternate means for capturing sunlight fully integrated with a battery, (2) a sustainable and economical anode material which will not be consumed as a part of the discharge reactions, and (3) an anode material that is free from loss of active materials, irreversible structural deformations, spontaneous deinsertion reactions, and safety concerns commonly encountered in the state of the art anode materials in ARBs. Projected photo battery does not require an external bias for revitalizing the active species and hence the discharge can be continued after a waiting period of 30 s. We used titanium nitride (TiN) as the photoanode, mainly because of its reported corrosion resistance in a wide variety of electrolytes, electrochemical stability, and sufficient conductivity, these properties already earned ceramic nitrides significant perspectives in fuel cell electrocatalysis, DSSC, biosensing, and so on.[20−23] This photo battery with a TiN photoanode is multifunctional in nature and it addresses critical issues such as longer charging time and higher charging voltage often encountered in typical energy storage devices apart from bringing in a sustainable photoanode for power production.

## 2. EXPERIMENTAL SECTION

**2.1. Materials.** Potassium ferricyanide, potassium ferrocyanide, potassium chloride, ferric chloride, and sulfuric acid were purchased from Alfa Aesar, India. All chemicals and reagents used were of analytical grade and used as received. Doubly distilled water was used for all the experiments.

**2.2. Preparation of Electrode Materials.** *Preparation KFe[Fe(CN)$_6$] (Fe$^{3+}$/Fe$^{2+}$) Supported on Carbon and Indium Tin Oxide (ITO).* KFe[Fe(CN)$_6$] (Fe$^{3+}$/Fe$^{2+}$) supported on carbon (1:4) was prepared by adding a solution of 20 mM K$_4$[Fe(CN)]$_6$ and 20 mM FeCl$_3$ into an aqueous suspension containing carbon particles. The KFe[Fe(CN)$_6$] (Fe$^{3+}$/Fe$^{2+}$) film was electrodeposited onto ITO-coated glass slide (8−12 Ω cm$^2$) using aqueous solution containing 20 mM K$_3$[Fe(CN)]$_6$, 20 mM FeCl$_3$, and 100 mM KCl. The electrochemical deposition was carried out by a three-electrode electrochemical cell using a potentiostat/galvanostat (CHI 660B), under a constant current density of 100 $\mu$A cm$^{-2}$ for 300 s.

*Preparation of TiN Electrode.* Cathodic arc deposition technique was used to prepare TiN electrode on thin flexible stainless steel sheets (SS-304). A vacuum of 10$^{-6}$ Torr was preserved before deposition in the Multi-Arc chamber used for deposition. Reactive nitrogen gas pressure was kept at 10 mTorr during the deposition of TiN and the substrate voltage was −200 V. TiN coating thickness on stainless steel was found to be 2−3 $\mu$m. TiN was coated on both sides of SS-304.

**2.3. Fabrication of Photo Battery.** Battery analysis were carried out in custom-made flooded cell (Supporting Information, Scheme S1). TiN film and KFe[Fe(CN)$_6$] (Fe$^{3+}$/Fe$^{2+}$) supported on carbon electrodes were cut into 2 × 2 cm$^2$ and attached to the sides of the cell, fabricated using polycarbonate sheets and quartz plates, and the distance between the two electrodes was maintained at <1 cm. A quartz plate was fitted on the photoanode side and the TiN electrode was held near the window using a clamp. Battery characterizations were done using KFe[Fe(CN)$_6$] (Fe$^{3+}$/Fe$^{2+}$) sup-

ported on carbon (1 mg cm$^{-2}$). Three M KCl (pH = 2) was used as the electrolyte and 1 M Na$_2$S$_2$O$_8$ was used as the chemical charging agent. Na$_2$S$_2$O$_8$ was present in the cell throughout the discharge−charge cycling unless otherwise specified. The discharge capacity was normalized with respect to the mass of KFe[Fe(CN)$_6$] (Fe$^{3+}$/Fe$^{2+}$). Halogen and tungsten lamps were used as the light sources.

**2.4. Characterization.** In situ UV−vis spectroelectrochemistry (PerkinElmer Lambda 950) was carried out in a quartz cuvette in two electrode configuration using KFe[Fe(CN)$_6$] (Fe$^{3+}$/Fe$^{2+}$)/ITO (150 $\mu$g/cm$^{-2}$) as the working electrode and TiN as the counter electrode. The % transmittance of KFe[Fe(CN)$_6$] (Fe$^{3+}$/Fe$^{2+}$)/ITO before and after short circuiting to a TiN electrode was measured in the UV−vis region in the presence and absence of Na$_2$S$_2$O$_8$. XRD of samples were measured using a Bruker D8 Advance. XPS spectrum of TiN was recorded using Thermo K-Alpha (Thermo Scientific, East Grinstead, U.K.) using a monochromatic Al K$\alpha$ source at 100 W. Charge−discharge measurements were carried out in a two-electrode configuration at a specific discharge current of 400 mA/g without any charging current using a CHI 660B electrochemical workstation. The cyclic voltammogram of KFe[Fe(CN)$_6$] (Fe$^{3+}$/Fe$^{2+}$) supported on a glassy carbon electrode was carried out using three-electrode systems with a Pt counter electrode and a saturated calomel reference electrode.
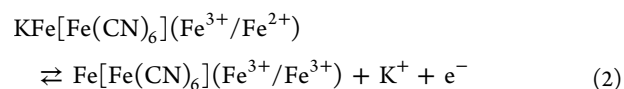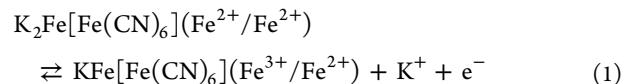
## ■ RESULTS AND DISCUSSION

The photo battery consists of a titanium nitride (TiN) photoelectrode, iron(III) hexacyanoferrate(II) (supported on carbon), which has been widely investigated as promising cathode material as the battery active species and 3 M KCl (pH = 2) electrolyte containing sodium persulfate (Na$_2$S$_2$O$_8$) as chemical battery charging agent (Scheme 1, see Experimental Section). Cyclic voltammogram of iron(III) hexacyanoferrate-(II) coated on glassy carbon electrode (Figure 1a), shows multiple redox states with the completely reduced form iron(II) hexacyanoferrate(II) (K$_2$Fe[Fe(CN)$_6$] (Fe$^{2+}$/Fe$^{2+}$) colorless), the partially oxidized form iron(III) hexacyanoferrate(II) (KFe[Fe(CN)$_6$] (Fe$^{3+}$/Fe$^{2+}$), intense blue) and completely oxidized form iron(III) hexacyanoferrate(III) (Fe[Fe(CN)$_6$] (Fe$^{3+}$/Fe$^{3+}$, green).[24−26] The associated redox reactions are given in eqs 1 and 2 and are accompanied by insertion and deinsertion of potassium ions back and forth the crystal lattice. XRD pattern of iron(III) hexacyanoferrate (II) is shown in Supporting Information, Figure S1, and it corresponds to the FCC crystal lattice where iron is coordinated to carbon and nitrogen in +2 and +3 oxidation states, respectively,[27,28] with mobile K$^+$ ions. Hence, this KFe[Fe(CN)$_6$] (Fe$^{3+}$/Fe$^{2+}$) system was chosen as the battery active species as it can reversibly undergo insertion and deinsertion of K$^+$ ions. TiN was chosen as the photoelectrode because of the presence of a native oxynitride layer[2,29−32] on its surface which can absorb visible part of the solar spectrum (Figure 1b) and its good electronic conductivity and high corrosion resistance.[33,34] TiN exhibited a broad absorption spectrum spanning the visible and UV regions making it a promising photoelectrode to harvest the visible light (Figure 1b). Kubelka−Munk plot (inset of Figure 1b) clearly showed band gap close to ∼2.2 eV, which falls in the region where the solar spectrum is intense.[35] X-ray diffraction (XRD) pattern and X-ray photoelectron spectroscopy (XPS) data of TiN are shown in Supporting Information, Figure S2, which unambiguously confirms the presence of TiN and titanium

**Scheme 1.** (a) Photo Battery in the Dark; (b) Discharge Reactions in the Presence of Light; (c) $Na_2S_2O_8$ Assisted Rapid Recovery of the Battery Active Species
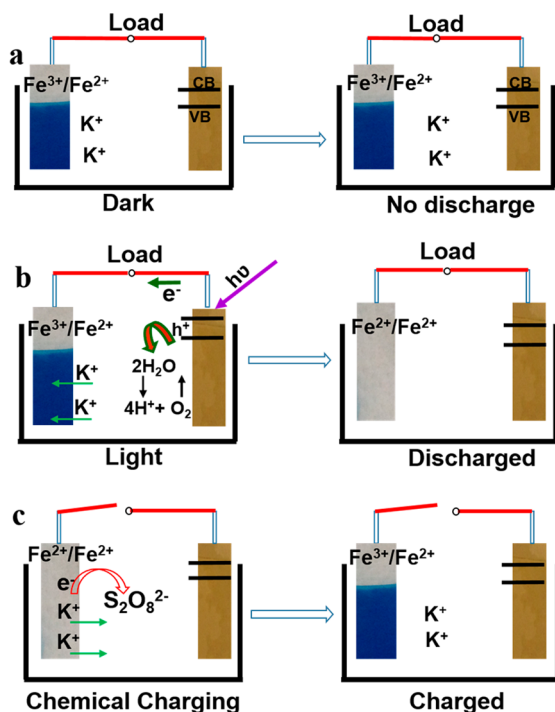


oxynitride (TiON) along with $TiO_2$. Surface oxidation of TiN could be responsible for the formation of TiON and $TiO_2$. This is in line with the previous reports where TiN coated by physical vapor deposition (PVD) invariably contained visible

light active titanium oxynitride.[29−33,36,37] It should be noted that TiN can be easily coated on stainless steel substrates by PVD and it does not require any post coating treatments to exhibit visible light activity. Further, the coexistence of visible light active TiON layer in combination with conducting TiN layer is expected to increase electron−hole separation and the charge propagation.

$$K_2Fe[Fe(CN)_6](Fe^{2+}/Fe^{2+})$$
$$\rightleftarrows KFe[Fe(CN)_6](Fe^{3+}/Fe^{2+}) + K^+ + e^- \qquad (1)$$

$$KFe[Fe(CN)_6](Fe^{3+}/Fe^{2+})$$
$$\rightleftarrows Fe[Fe(CN)_6](Fe^{3+}/Fe^{3+}) + K^+ + e^- \qquad (2)$$

The working principle involves the light assisted generation of electron−hole pairs in TiON/TiN and the pumping of generated photoelectrons to $KFe[Fe(CN)_6]$ $(Fe^{3+}/Fe^{2+})$, causing its reduction to $(K_2Fe[Fe(CN)_6]$ $(Fe^{2+}/Fe^{2+})$, with simultaneous $K^+$ ion insertion (for charge balance), thereby generating power (Scheme 1). We believe that at this step the generated holes will be used for oxidizing water to $O_2$ as a balancing reaction. Preliminary evidence for oxygen bubble formation during the discharge is shown in Supporting Information, Figure S3. For a single cell (in the ambient light) obtained open circuit voltage (OCV) was ∼1.1 V (Figure 1c), and the measured half-cell OCV of $KFe[Fe(CN)_6]$ $(Fe^{3+}/Fe^{2+})$, and TiN were ∼1.12 V and ∼16 mV versus RHE (in 3 M KCl, pH = 2), respectively. The equilibrium $H_2$ reduction potential at pH 2 is −118 mV and thus the sufficiently positive value of 16 mV obtained with TiN makes it an attractive anode material without having the issue of $H_2$ evolution observed on many existing anodes.[19] In the dark, OCV obtained was ∼0.74
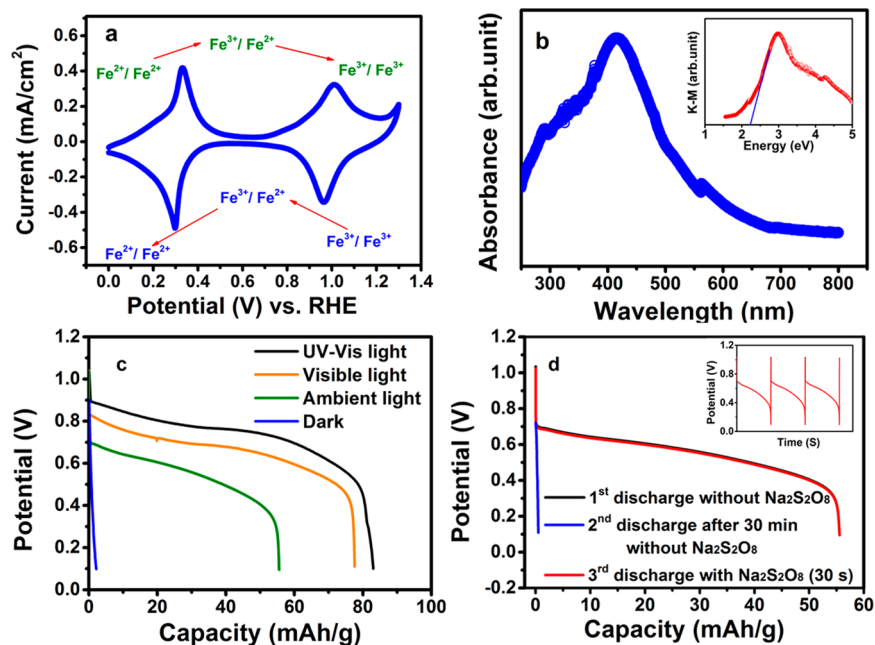


**Figure 1.** (a) Cyclic voltammogram of $KFe[Fe(CN)_6]$ $(Fe^{3+}/Fe^{2+})$ coated on glassy carbon electrode in 3 M KCl (pH = 2) at a scan rate of 100 mV/s. (b) UV−vis spectrum of TiN (inset shows the transformed Kubelka−Munk plot), showing the broad absorption spectrum of TiN spanning the visible and UV regions. (c) Discharge curves of photo battery in the presence and absence of light at a rate of 400 mA/g. (d) Continuous discharge behavior (rate 400 mA/g) in the ambient light with and without $Na_2S_2O_8$ without applying any external charging current. Inset shows the multiple charge−discharge behavior with $Na_2S_2O_8$ in the ambient light without any charging current. Different colors in the plot are explained in the text.
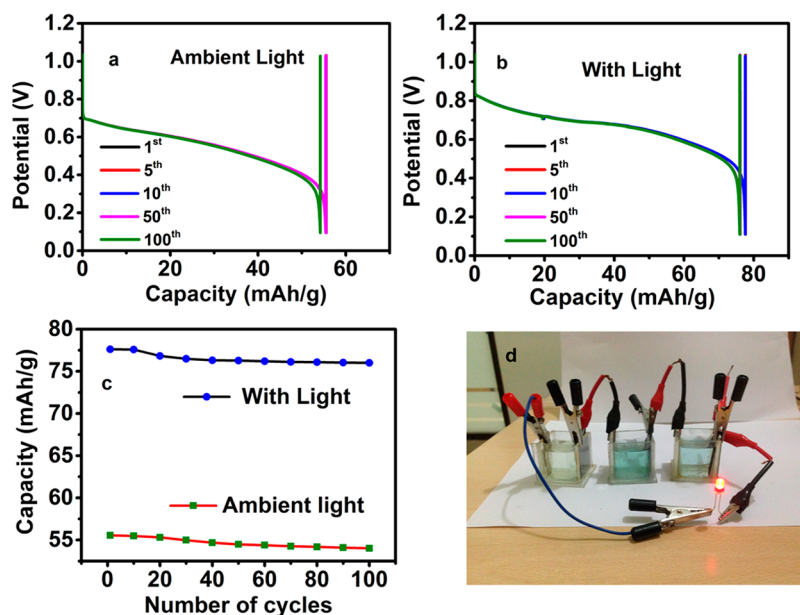
**Figure 2.** Cycling performance of photo battery at 400 mA/g: (a) in the ambient light; (b) intentionally shined light (visible light, 35 mW/cm$^2$); (c) capacity vs cycle number; (d) image of photo battery powering a LED. No charging current was used for these experiments.

V, and when intentionally shined light (visible light source, 35 mW cm$^{-2}$), the cell OCV shot up to ~1.2 V, suggesting unambiguously that the battery chemistry is visible light driven. pH of the electrolyte was optimized as shown in the Supporting Information, Figure S4, and the electrolyte composition that delivered the highest OCV in the ambient light was chosen for subsequent studies. From a single cell in the presence of light (intentionally shined, visible light), the discharge capacity obtained was 77.8 mAh/g with a higher discharge plateau (Figure 1c). In the dark negligible capacity with an inferior discharge plateau were obtained and in the presence of ambient light, discharge capacity significantly improved to 55.5 mAh/g, which is ~72% of the artificial light assisted capacity. When a UV−vis light source was employed, the discharge pleateau and capacity improved further (black line, Figure 1c), suggesting the involvement of TiO$_2$ along with TiON in the discharge process. The negligible capacity observed in the dark can be utilized for preventing the self-discharge, if the battery optical window is provided with a proper shutter. The decreased discharge capacity in the ambient light (compared to intentionally shined discharge capacity) could be due to the lowered density of photogenerated electrons, electron−hole recombination, and so on; however, these require independent experimental verification and are under investigation. After the first discharge, the system was left at the open circuit for 30 min (without Na$_2$S$_2$O$_8$), and the subsequent attempt to discharge the cell gave very inferior capacity, Figure 1d (blue line), however, when the cell was supplemented with Na$_2$S$_2$O$_8$, KFe[Fe(CN)$_6$] (Fe$^{3+}$/Fe$^{2+}$) redox state was rapidly restored (in 30 s) because of the oxidizing action of Na$_2$S$_2$O$_8$ on (K$_2$Fe[Fe(CN)$_6$] (Fe$^{2+}$/Fe$^{2+}$), as shown in Scheme 1c (corresponding movies are available in Supporting Information, Movies 1a,b), and the discharge could be continued without any electrical input and furnished similar capacity as in the first cycle (Figure1d, red and black lines). The similar discharge capacities obtained with and without Na$_2$S$_2$O$_8$ (Figure 1d) manifest that Na$_2$S$_2$O$_8$ does not affect the discharge chemistry occurring at the cathode and is mainly acting as a chemical charging agent. This is further clear

from the similar OCV profiles obtained with Na$_2$S$_2$O$_8$ (Supporting Information, Figure S5). We would like to emphasize that it is not our aim to accelerate the discharge process using light but to suggest a possible remedy for the funadmental scientific challenges faced by the existing anode materials in ARBs by bringing in a sustainable photoanode.

During this spontaneous chemical charging, persulfate was reduced to SO$_4^{\bullet-}$ and SO$_4^{2-}$, in line with the previously established reduction products of Na$_2$S$_2$O$_8$.[38] For the subsequent cycles during the discharge, given the fact that SO$_4^{\bullet-}$ is a very good hole scavenger,[39] it is believed that water oxidation step will be replaced by the hole scavenging of SO$_4^{\bullet-}$ to some extent. If oxygen evolution does take place at the anode during the discharge, it should be accompanied by a pH decrease in the cell based on the reaction, 2H$_2$O → 4H$^+$ + O$_2$. To probe the chemistry at the anode further, we carried out pH and OCV measurements after discharge-chemical charge cycles, Supporting Information, Figure S6, and only a little change in pH and OCV were observed. This implicates that the generated protons during oxygen evolution could be used up by Na$_2$S$_2$O$_8$ during the chemical charging step as shown in eq 7. When KFe[Fe(CN)$_6$] (Fe$^{3+}$/Fe$^{2+}$) loading was increased, a concomitant increase in discharge time was observed (Supporting Information, Figure S7). Further, an attempt to discharge the cell with a TiO$_2$ photoelectrode (in the ambient light) resulted in a negligible discharge capacity with an inferior OCV (Supporting Information, Figure S8, and corresponding Supporting Information, Movie 2). The capacity and OCV did not reveal any significant change even after the TiO$_2$ photoelectrode surface was intentionally shined (visible light, 35 mW/cm$^2$). All these proved beyond doubt that KFe[Fe-(CN)$_6$] (Fe$^{3+}$/Fe$^{2+}$) is the battery active species, Na$_2$S$_2$O$_8$ is inevitable for charging the battery without an external bias and TiON/TiN is mainly involved in harvesting the ambient light.

Proposed half-cell reactions are shown below and it involves light-assisted reduction and Na$_2$S$_2$O$_8$ assisted recovery of KFe[Fe(CN)$_6$] (Fe$^{3+}$/Fe$^{2+}$). As revitalizing the battery takes only 30 s when left at open circuit because of the oxidizing
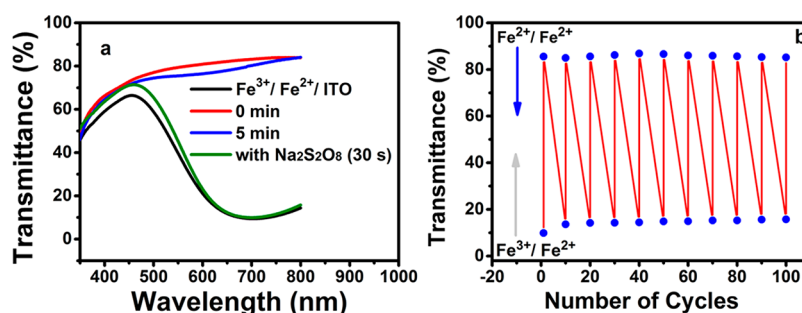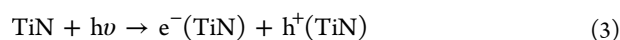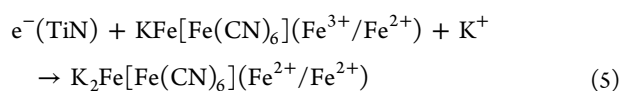
**Figure 3.** (a) In situ UV−vis spectra with and without $Na_2S_2O_8$ exhibiting light assisted reduction and $Na_2S_2O_8$ assisted recovery of $KFe[Fe(CN)_6]$ ($Fe^{3+}/Fe^{2+}$) coated on ITO (different colors in the plot are explained in the text). (b) UV−vis cycling performance (@670 nm) of photo battery with $Na_2S_2O_8$.

action of $Na_2S_2O_8$, the charging time required was significantly reduced. This rapid revitalization without an external bias addresses the major concerns of longer charging time and higher charging voltage required in typical energy storage devices.
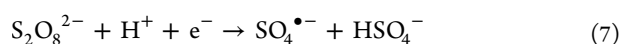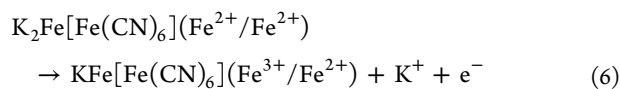
Anodic reactions:

$$TiN + h\upsilon \rightarrow e^-(TiN) + h^+(TiN) \qquad (3)$$

$$h^+ + 2H_2O \rightarrow O_2 + 4H^+ \qquad (4)$$

Cathodic reactions:

$$e^-(TiN) + KFe[Fe(CN)_6](Fe^{3+}/Fe^{2+}) + K^+$$
$$\rightarrow K_2Fe[Fe(CN)_6](Fe^{2+}/Fe^{2+}) \qquad (5)$$

Chemical charging reactions:

$$K_2Fe[Fe(CN)_6](Fe^{2+}/Fe^{2+})$$
$$\rightarrow KFe[Fe(CN)_6](Fe^{3+}/Fe^{2+}) + K^+ + e^- \qquad (6)$$

$$S_2O_8{}^{2-} + H^+ + e^- \rightarrow SO_4{}^{\bullet-} + HSO_4{}^- \qquad (7)$$

$Na_2S_2O_8$ assisted voltage recovery of the photo battery for different cycles in the ambient light and intentionally shined light are shown in Figure 2a and b, respectively. The battery active species got quickly revitalized in 30 s, as shown by the sudden jump of the voltage profiles at the end of every discharge and the discharge could be continued further without an external bias. The stability of the photo battery is shown in Figure 2c. The capacity remained approximately stable for more than 100 cycles, retaining 97.9% of its initial capacity at the end of 100 cycles, suggesting a sustainable power generation. In ambient light we could power a LED using the photo battery (Figure 2d and corresponding Supporting Information, Movie 3). Further, we followed the stability of TiN photoanode by XRD techniques to understand the most crucial aspect of its structural integrity to function as a sustainable anode. The results showed almost identical XRD patterns (Supporting Information, Figure S9) before and after cycling (for 100 cycles), revealing its decent stability and cyclability. It should be noted that the role of $Na_2S_2O_8$ is that of a sacrificial agent and is consumed irreversibly; therefore, the proposed photo battery is not truly a rechargeable battery and the cell requires a $Na_2S_2O_8$ supplement when it is exhausted. However, $Na_2S_2O_8$ is an inexpensive chemical, and hence, cell charge dependence on $Na_2S_2O_8$ will not have major cost implications. Further the chemical charging strategy is expected to circumvent the

structural changes of cathodes and electrolyte decomposition commonly encountered in electrically rechargeable batteries.

To further understand the system, we carried out in situ UV−vis spectroelectrochemistry with $KFe[Fe(CN)_6]$ ($Fe^{3+}/Fe^{2+}$) coated ITO ($KFe[Fe(CN)_6]$ ($Fe^{3+}/Fe^{2+}$)/ITO) and a TiN photoelectrode. As shown in Figure 3a, when TiN was short circuited to $KFe[Fe(CN)_6]$ ($Fe^{3+}/Fe^{2+}$)/ITO, % transmittance of $KFe[Fe(CN)_6]$ ($Fe^{3+}/Fe^{2+}$)/ITO around 500−800 nm was significantly increased due to its reduction to ($K_2Fe[Fe(CN)_6]$ ($Fe^{2+}/Fe^{2+}$; red line). Similar changes in optical contrast were reported earlier under electrical inputs for $KFe[Fe(CN)_6]$ ($Fe^{3+}/Fe^{2+}$)/ITO and is due to intervalence charge transfer.[39] In the absence of $Na_2S_2O_8$, conversion of $KFe[Fe(CN)_6]$ ($Fe^{3+}/Fe^{2+}$) to ($K_2Fe[Fe(CN)_6]$ ($Fe^{2+}/Fe^{2+}$) was observed when TiN was short circuited to $KFe[Fe(CN)_6]$ ($Fe^{3+}/Fe^{2+}$)/ITO electrode (red line); however, when left at the open circuit, the regeneration did not happen even after 5 min waiting time (blue line). However, when $Na_2S_2O_8$ was added to the system, in line with previously discussed battery charge−discharge behavior, the $KFe[Fe(CN)_6]$ ($Fe^{3+}/Fe^{2+}$) redox state was restored in 30 s (green line, Figure 3a), and the optical modulation could be continued further (Figure 3b). This investigation reveals that in the absence of $Na_2S_2O_8$, only the electron pumping occurred from TiN photoelectrode to $KFe[Fe(CN)_6]$ ($Fe^{3+}/Fe^{2+}$) without its regeneration and, hence, the system could do only one optical modulation, and hence, it behaved like a primary battery. These reinforce the fact that, for the device to be a secondary battery (chargeable) without electrical input, $Na_2S_2O_8$ is indeed required.

The optical modulation versus cycle number is shown in Figure 3b with $Na_2S_2O_8$. As shown, the device can be cycled with higher optical contrast for over 100 cycles (after 100 cycles, 91.8% of transmittance is retained) clearly demonstrating the stability and efficiency of the device. The optical contrast and the efficiency of different cycles extracted from UV−vis spectra are shown in Table 1. The faster optical switching and a stable response for over 100 cycles with higher optical contrast of the order of 91.8% without the aid of an

**Table 1. Optical Modulation Data Extracted from UV−Vis Spectra**

| cycle number | optical contrast (%) | efficiency |
|---|---|---|
| 1st | 75.69 | |
| 10th | 71.33 | 94.23 |
| 50th | 71.06 | 93.88 |
| 100th | 69.49 | 91.80 |

external bias is something unique and is due to the carefull choice of architectural components. These results are coherent with our battery results and unambiguously support our conclusion that battery discharge chemistry is light driven and charge chemistry is $Na_2S_2O_8$ driven.

To further understand the mechanism of $KFe[Fe(CN)_6]$ $(Fe^{3+}/Fe^{2+})$ reduction and oxidation in the presence of ambient light, we carried out several experiments by selecting different types of electron acceptors using TiN as the photoelectrode. In the presence of $H_2O_2$, no $KFe[Fe(CN)_6]$ $(Fe^{3+}/Fe^{2+})$ reduction was observed, suggesting that $H_2O_2$ competes with $KFe[Fe(CN)_6]$ $(Fe^{3+}/Fe^{2+})$ for photogenerated electrons (corresponding Supporting Information, Movie 4). This is not surprising given the electron accepting capability of $H_2O_2$ in photo (electro) catalysis.[36] When we used an Al electrode (without $H_2O_2$) in place of TiN that can inherently pump electrons without the aid of light (because of its negative standard reduction potential of $-1.66$ V), immediate reduction of $KFe[Fe(CN)_6]$ $(Fe^{3+}/Fe^{2+})$ was observed. However, in the presence of $H_2O_2$, as in the case of TiN electrode, no reduction was observed, suggesting that $H_2O_2$ accepts the electrons from Al causing its dissolution (corresponding video is available in Supporting Information, Movie 5a,b). In line with these results, in $H_2O_2$ supplemented photo battery with TiN photoelectrode, discharge capacity was very inferior (Supporting Information, Figure S10). Further, Al electrode could cause the reduction of $KFe[Fe(CN)_6]$ $(Fe^{3+}/Fe^{2+})$ in the presence of $Na_2S_2O_8$, suggesting that $Na_2S_2O_8$ does not compete (like $H_2O_2$) with $KFe[Fe(CN)_6]$ $(Fe^{3+}/Fe^{2+})$ for electrons from Al (corresponding video is available in Supporting Information, Movie 6). Therefore, we believe that in the photo battery, $Na_2S_2O_8$ functions mainly as a chemical charging agent (in situ chemical oxidation of $(K_2Fe[Fe(CN)_6]$ $(Fe^{2+}/Fe^{2+})$ to $KFe[Fe(CN)_6]$ $(Fe^{3+}/Fe^{2+}))$. It may compete for photogenerated electrons to some extent at the photoelectrode/electrolyte interface; however the reported hole scavenging ability of $SO_4^{\bullet-}$ radical species[38] existing at the interface may allow the electrons to be pumped to $KFe[Fe(CN)_6]$ $(Fe^{3+}/Fe^{2+})$ generating power. Therefore, in the photo battery, photogenerated electrons are responsible for the battery discharge chemistry and $Na_2S_2O_8$ is responsible for the battery charge chemistry.

## 3. CONCLUSIONS

In conclusion, we have successfully demonstrated ambient light assisted power production in a battery wherein light is used as the anode to actuate discharge reactions in its cathode. By employing a range of techniques, it is proved that the battery discharge chemistry is light driven and charge chemistry is $Na_2S_2O_8$ driven without the aid of any external power input. This methodology of using a photoanode leads to alternate means for capturing sunlight fully integrated with a battery which in turn is free from dissolution of active materials, irreversible structural changes and spontaneous deinsertion reactions commonly encountered in the state of the art anode materials in ARBs. This sustainable device addresses critical issues such as longer charging time, requirement of charging voltage and higher self-discharge rate often encountered in typical energy storage devices. It is not our intention to accelerate the discharge process using light, but to suggest a possible remedy for the funadmental scientific challenges faced by the existing anode materials in ARBs by bringing in a sustainable photoanode. Cell revitalization dependence on $Na_2S_2O_8$ may be questioned, however, its low cost is not expected to have major cost implications. Questions may arise on its applicability in the night time, however, since the battery works using ambient light, it may be able to produce power even in the presence of street light, household lighting, indoor lighting, and so on. The possibilities of self-regeneration using chemical charging agents open avenues for continuous power production in the likely events of electrical input unavailability for revitalizing the energy storage device.

## ■ ASSOCIATED CONTENT

### ⓢ Supporting Information

XRD of $KFe[Fe(CN)_6]$ $(Fe^{3+}/Fe^{2+})$, XRD of TiN before and after cycling, XPS of TiN, observation of oxygen bubbles on TiN anode, OCV vs pH plot, OCV profile of photo battery with $Na_2S_2O_8$, pH and OCV profile vs number of cycles plot, discharge curves of photo battery with different loading of $KFe[Fe(CN)_6]$ $(Fe^{3+}/Fe^{2+})$, discharge curve of $TiO_2$ anode-based photo battery, and discharge curve of photo battery with $H_2O_2$. The Supporting Information is available free of charge on the ACS Publications website at DOI: 10.1021/acs.jpcc.5b02871.

## ■ AUTHOR INFORMATION

### Corresponding Author
*E-mail: musthafa@iiserpune.ac.in. Phone: +912025908261.

### Notes
The authors declare no competing financial interest.

## ■ REFERENCES

(1) Wang, W.; Chen, J.; Li, C.; Tian, W. Achieving Solar Overall Water Splitting With Hybrid Photosystems of Photosystem II and Artificial Photocatalysts. *Nat. Commun.* 2014, *5*, 1−8.

(2) Pan, C.; Takata, T.; Nakabayashi, M. A Complex Perovskite-Type Oxynitride: The First Photocatalyst for Water Splitting Operable at up to 600 nm. *Angew. Chem., Int. Ed.* 2015, *54*, 1−6.

(3) Jacobson, M. Z. Review of Solutions to Global Warming, Air Pollution, and Energy Security. *Energy Environ. Sci.* 2009, *2*, 148−173.

(4) Hoel, M.; Kverndokk, S. Depletion of Fossil Fuels and the Impacts of Global Warming. *Resour. Energy Econ.* 1996, *18*, 115−136.

(5) Leif, H.; Sharon, S. Artificial Photosynthesis and Solar Fuels. *Acc. Chem. Res.* 2009, *42*, 1859−1860.

(6) Dar, M. I.; Arora, N.; Gao, P.; Ahmad, S.; Gra, M. Investigation Regarding the Role of Chloride in Organic − Inorganic Halide Perovskites Obtained from Chloride Containing Precursors. *Nano Lett.* 2014, *14*, 6991−6996.

(7) Bonraccorso, F. Graphene, Related Two-Dimensional Crystals, and Hybrid Systems for Energy Conversion and Storage. *Science* 2015, *347*, 1246501−1−9.

(8) Chueh, W. C.; Abbott, M.; Scipio, D.; Haile, S. M. High-Flux Solar-Driven Thermochemical Dissociation of $CO_2$ and $H_2O$ Using Ceria Redox Reactions. *Science* 2010, *63*, 1797−1801.

(9) Steven, R. Y.; Jonathan, A. H.; Kimberly, S.; Thomas, D. J.; Arthur, J. E.; Daniel, G. N. Wireless Solar Water Splitting Using Silicon-Based Semiconductors and Earth-Abundant Catalysts. *Science* 2011, *334*, 645−648.

(10) Goodenough, J. B.; Kim, Y. Challenges for Rechargeable Batteries. *J. Power Sources* 2011, *196*, 6688−6694.

(11) Larcher, D.; Tarascon, J. M. Towards Greener and More Sustainable Batteries for Electrical Energy Storage. *Nat. Chem.* 2015, *7*, 19−29.

(12) Meyer, M.; Cyril, V. C.; Lydie, V. B.; Ahmad, M.; Olivier, F.; Eleonore, M.; Sophie, M.; Jean, M. C.; Laurent, C.; Andre, V. Single-Ion Conductor Nanocomposite Organic−Inorganic Hybrid Membranes for Lithium Batteries. *J. Mater. Chem. A* **2014**, *2*, 12162−12165.

(13) Dunst, A.; Epp, V.; Hanzu, I.; Freunberger, S. A.; Wilkening, M. Short-Range Li Diffusion vs. Long-Range Ionic Conduction in Nanocrystalline Lithium Peroxide $Li_2O_2$ - the Discharge Product in Lithium-Air Batteries. *Energy Environ. Sci.* **2014**, *7*, 2739−2752.

(14) Cheng, H.; Scott, K. Selection of Oxygen Reduction Catalysts for Rechargeable Lithium-Air Batteries - Metal or Oxide? *Appl. Catal., B* **2011**, *108−109*, 140−151.

(15) Vanýsek, P. Electrochemical Series. In *Handbook of Chemistry and Physics*, 93rd ed.; Haynes, W. M., Ed.; CRC Press: New York, 2012; pp 5−80, ISBN 13:978-1-4398-8049-4.

(16) Abraham, K. M. Prospects and Limits of Energy Storage in Batteries. *J. Phys. Chem. Lett.* **2015**, *6*, 830−844.

(17) Haegyeom, K.; Kang, K. Aqueous Rechargeable Li and Na Ion Batteries. *Chem. Rev.* **2014**, *114*, 11788−11827.

(18) Xianyong, W.; Cao, Y.; Ai, X.; Qian, J.; Yang, H. A Low-Cost and Environmentally Benign Aqueous Rechargeable Sodium-Ion Battery Based on $NaTi_2(PO_4)_3$−$Na_2NiFe(CN)_6$ Intercalation Chemistry. *Electrochem. Commun.* **2013**, *31*, 145−148.

(19) Hyun, W. L.; Wang, R. Y.; Pasta, M.; Lee, S. W.; Liu, N.; Cui, Yi. Manganese Hexacyanomanganate Open Framework as a High-Capacity Positive Electrode Material for Sodium-Ion Batteries. *Nat. Commun.* **2014**, *5*, 1−6.

(20) Haifeng, L.; Shichun, M. Nano-Ceramic Support Materials for Low Temperature Fuel Cell Catalysts. *Nanoscale* **2014**, *6*, 5063−5074.

(21) Ravikumar, T.; Sivakumar, P.; Bruno, G. P.; Scott, K. Nafion-Stabilised Platinum Nanoparticles Supported on Titanium Nitride: An Efficient and Durable Electrocatalyst for Phosphoric Acid based Polymer Electrolyte Fuel Cells. *Electrochim. Acta* **2013**, *109*, 365−369.

(22) Shanmu, D.; Xiao, C.; Lin, G.; Guanglei, C.; Lixue, Z.; Xinhong, Z.; Zhihong, L.; Pengxian, H.; Hongxia, X.; Jianhua, Y.; et al. A Biocompatible Titanium Nitride Nanorods Derived Nanostructured Electrode for Biosensing and Bioelectrochemical Energy Conversion. *Biosens. Bioelectron.* **2011**, *26*, 4088−4094.

(23) Chuan-Pei, L.; Lu-Yin, L.; Vittal, R.; Kuo-Chuan, H. Favourable Effects of Titanium Nitride or Its thermally Treated Version in a Gel Electrolyte for a Quasi-Solid-State Dye-Sensitized Solar Cell. *J. Power Sources* **2011**, *196*, 1665−1670.

(24) Karyakin, A. A Prussian Blue and its Analogues: Electrochemistry and Analytical applications. *Electroanalysis* **2001**, *13*, 813−819.

(25) Neff, D. Electrochemistry of Polynuclear Transition Metal Cyanides: Prussian Blue and its Analogues. *Acc. Chem. Res.* **1986**, *19*, 162−168.

(26) Bleuzen, A. Photoinduced Ferrimagnetic Systems in Prussian Blue Analogues $C^I_xCo_4[Fe(Cn)_6]_{(y)}$ ($C^I$ = alkali cation). 1. Conditions to Observe the Phenomenon. *J. Am. Chem. Soc.* **2000**, *122*, 6648−6652.

(27) Buser, H. J.; Schwarzenbach, D.; Petter, W.; Ludi, A. The Crystal Structure of Prussian Blue: $Fe_4[Fe(CN)_6]_3 \cdot xH_2O$. *Inorg. Chem.* **1977**, *16*, 2704−2710.

(28) Widmann, A. Structure, Insertion Electrochemistry, and Magnetic Properties of a New Type of Substitutional Solid Solutions of Copper, Nickel, and Iron Hexacyanoferrates/Hexacyanocobaltates. *Inorg. Chem.* **2002**, *41*, 5706−5715.

(29) Abe, R.; Higashi, M.; Domen, K. Facile Fabrication of an Efficient Oxynitride TaON Photoanode for Overall Water Splitting into $H_2$ and $O_2$ Under Visible Light Irradiation. *J. Am. Chem. Soc.* **2010**, *132*, 11828−11829.

(30) Claire, L. P.T.; Akio, I.; Ahmed, Z.; Laurent, L. G.; Masaaki, Y.; Jun, K.; Franck, T.; Kazunari, D. Photoelectrochemical Properties of Crystalline Perovskite Lanthanum Titanium Oxynitride Films Under Visible Light. *J. Phys. Chem. C* **2009**, *113*, 6156−6162.

(31) Saha, N. C.; Tompkins, H. G. Titanium Nitride Oxidation Chemistry: An X-ray Photoelectron Spectroscopy Study. *J. Appl. Phys.* **1992**, *72*, 3072−3079.

(32) Martínez, F. E.; Sakatani, Y. C.; Boissiere, C.; Grosso, D.; Fuerts, A.; Fraxidas, J.; Sanchez, C. Nanostructured Titanium Oxynitride Porous Thin Films as Efficient Visible-Active Photocatalysts. *Adv. Funct. Mater.* **2007**, *17*, 3348−3354.

(33) Ray, W.Y. P.; Joan, P.Y. H.; Xuanyong, L.; Chung, C. Y.; Paul, K. C.; Kelvin, W. K. Y.; William, W. L.; Kenneth, M. C. C. Formation of Titanium Nitride Barrier Layer in Nickel−Titanium Shape Memory Alloys by Nitrogen Plasma Immersion Ion Implantation for Better Corrosion Resistance. *Thin Solid Films* **2005**, *488*, 20−25.

(34) Starosvetsky, D.; Gotman, I. Corrosion Behavior of Titanium Nitride Coated Ni-Ti Shape Memory Surgical Alloy. *Biomaterials* **2001**, *22*, 1853−1859.

(35) Hebrink, T. J. Durable Polymeric Films for Increasing the Performance of Concentrators. In *Third Generation Photovoltaics*; Fthenakis, V., Ed.; InTech: Rijeka, Croatia, 2012; Chapter 8. ISBN: 978-953-51-0304-2.

(36) Milošv, I.; Strehblow, H. H.; Navinšek, B.; Metikoš, H. M. Electrochemical and Thermal Oxidation of TiN Coatings Studied by XPS. *Surf. Interface Anal.* **1995**, *23*, 529−539.

(37) Ottakam, T. M. M.; Ravikumar, T.; Sampath, S. Platinum Particles Supported on Titanium Nitride: an Efficient Electrode Material for the Oxidation of Methanol in Alkaline Media. *J. Mater. Chem.* **2010**, *20*, 10643−10651.

(38) Mills, A.; Valenzuela, M. A. Photo-Oxidation of Water Sensitized by $TiO_2$ and $WO_3$ in Presence of Different Electron Acceptors. *Rev. Mex. Fis.* **2004**, *50*, 287−296.

(39) Memming, R. Mechanism of the Electrochemical Reduction of Persulfates and Hydrogen Peroxide. *J. Electrochem. Soc.* **1969**, *116*, 785.